


Inhibition of P2X7 receptors improves outcomes after traumatic brain injury in rats

Xiaofeng Liu¹ · Zhengqing Zhao² · Ruihua Ji³ · Jiao Zhu¹ · Qian-Qian Sui¹ · Gillian E. Knight⁴ · Geoffrey Burnstock^{4,5} · Cheng He¹ · Hongbin Yuan³ · Zhenghua Xiang¹ 

Received: 9 December 2016 / Accepted: 3 August 2017 / Published online: 19 August 2017
© Springer Science+Business Media B.V. 2017

Abstract Traumatic brain injury (TBI) is the leading cause of death and disability for people under the age of 45 years worldwide. Neuropathology after TBI is the result of both the immediate impact injury and secondary injury mechanisms. Secondary injury is the result of cascade events, including glutamate excitotoxicity, calcium overloading, free radical generation, and neuroinflammation, ultimately leading to brain cell death. In this study, the P2X7 receptor (P2X7R) was detected predominately in microglia of the cerebral cortex and was up-regulated on microglial cells after TBI. The microglia transformed into amoeba-like and discharged many microvesicle (MV)-like particles in the injured and adjacent regions. A P2X7R antagonist (A804598) and an immune inhibitor (FTY720) reduced significantly the number of MV-like particles in the injured/adjacent regions and in cerebrospinal fluid, reduced the number of neurons undergoing apoptotic cell death, and increased the survival of neurons in the cerebral cortex injured and adjacent regions. Blockade of the

P2X7R and FTY720 reduced interleukin-1 β expression, P38 phosphorylation, and glial activation in the cerebral cortex and improved neurobehavioral outcomes after TBI. These data indicate that MV-like particles discharged by microglia after TBI may be involved in the development of local inflammation and secondary nerve cell injury.

Keywords Traumatic brain injury · P2X7R · Microglial cells · Microvesicles · Neuroinflammation

Introduction

Traumatic brain injury (TBI) is the leading cause of death and disability for people under the age of 45 years [1]. Worldwide, about ten million people are annually admitted to hospital after TBI. An estimated 57 million people have survived brain injury [2]. Neuropathology after TBI is the result of both the

X Liu, Z Zhao and R Ji contributed equally to this work should be considered as co-first authors.

Electronic supplementary material The online version of this article (doi:10.1007/s11302-017-9579-y) contains supplementary material, which is available to authorized users.

✉ Hongbin Yuan
jfczyy@aliyun.com

✉ Zhenghua Xiang
xiang-zhenghua@163.com

¹ Department of Neurobiology, MOE Key Laboratory of Molecular Neurobiology, Ministry of Education, Neuroscience Research Centre of Changzheng Hospital, Second Military Medical University, Shanghai 200433, People's Republic of China

² Department of Neurology, Neuroscience Research Center of Changzheng Hospital, Second Military Medical University Shanghai, Yangpu Qu, People's Republic of China

³ Department of Anesthesiology, Changzheng Hospital, Second Military Medical University, 415 Fengyang Road, Shanghai 200003, People's Republic of China

⁴ Autonomic Neuroscience Centre, University College Medical School, Rowland Hill Street, London NW3 2PF, UK

⁵ Department of Pharmacology, Melbourne University, Parkville, Australia

immediate impact injury and secondary injury mechanisms [3]. The immediate impact injury occurs at the time of exposure to the external force [4, 5]. Secondary injury occurs from

minutes to months after TBI and is the result of cascade events that ultimately lead to brain cell death, tissue damage, and atrophy [6]. These cascade events include glutamate

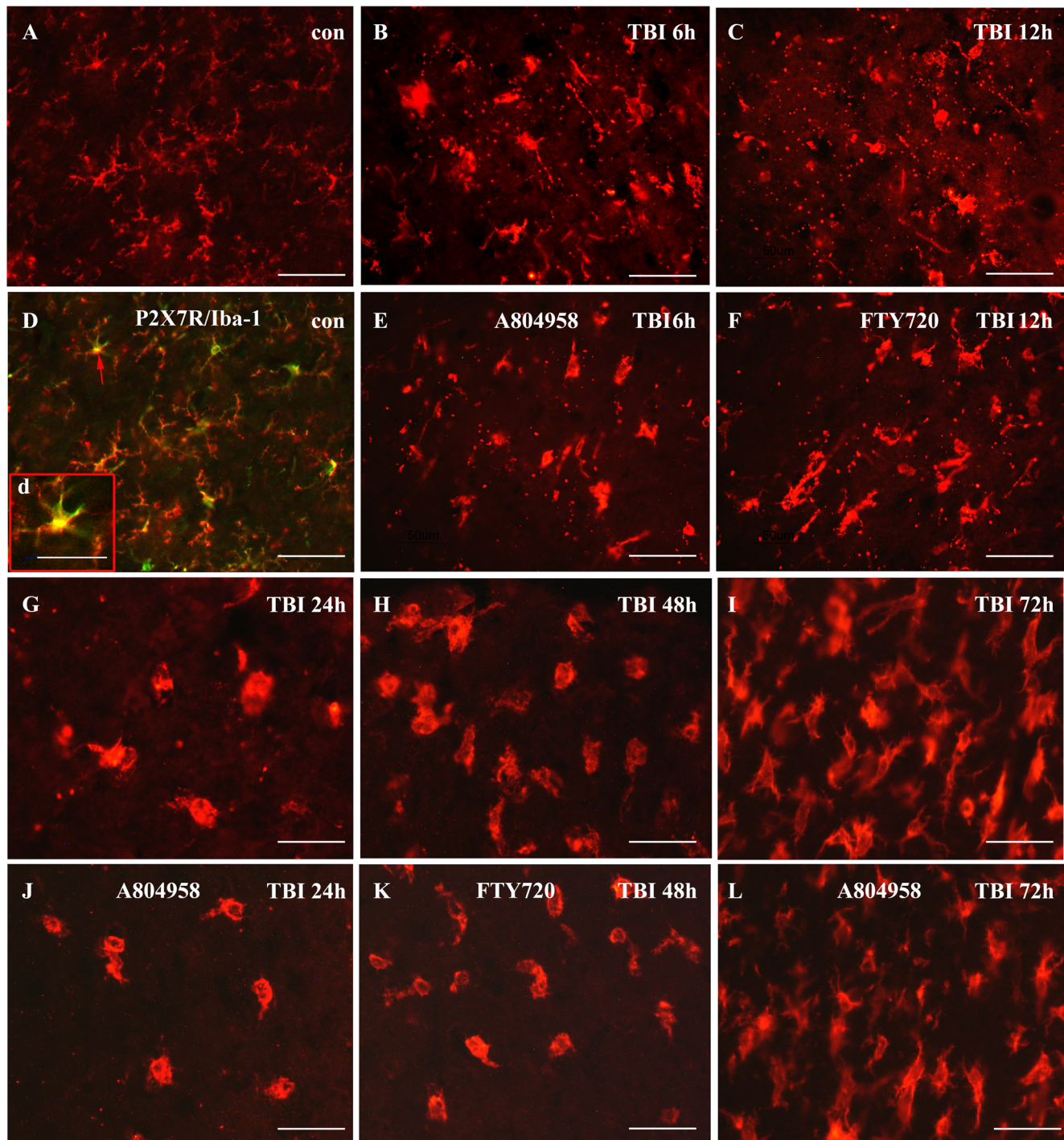


Fig. 1 Expression of P2X7R-ir (red) in the cerebral cortex of control and TBI rats. Subpanel **a** is P2X7R-ir and subpanel **d** is an immersed image from **a** (red) and Iba-1-ir (green, a marker for microglial cell) from the control group. Note that almost all the P2X7R-ir are also labeled with Iba-1. The immunostaining results show that P2X7R-ir is predominately expressed in microglial cells. **b, c, g, h, i** P2X7R-ir from the TBI groups at 6, 12, 24, 48, and 72 h, respectively. **e, j, l, f, k** P2X7R-ir from TBI+

A804598 and TBI+FTY720 groups. Note that microvesicle (MV)-like particles were detected mainly at 6 and 12 h after TBI, and A804598 and FTY720 decreased the number of vesicles. In the early stages from 6 to 24 h after TBI, the number of P2X7R-ir microglial cells did not change significantly but increased from 48 h after TBI. Both A804598 and FTY720 decreased the number of microglia cells significantly at 96 h after TBI. All scale bars = 60 μ m

excitotoxicity, perturbation of cellular calcium homeostasis, increased free radical generation and lipid peroxidation, mitochondrial dysfunction, and neuroinflammation [7]. The relative contributions of these different cascade events to the secondary injury remain to be determined. In addition to the excitatory amino acid glutamate, extracellular ATP acts as an important signal molecule in the processes of central nervous system (CNS) injury and is currently attracting more attention [8–12]. There is a high concentration of extracellular ATP at the injured and adjacent regions of TBI that may be involved in the secondary injury after TBI. There is currently no information available about this.

Microvesicles (MV) are small (0.1–1 μm) vesicles which bud directly from the plasma membrane of many brain cell types and are released into the extracellular environment and regulate the functional activity of other cells. This is a novel method of cell-to-cell communication [13, 14]. Previous data showed that ATP can trigger MV shedding and interleukin (IL)-1 β release from both microglia and astrocytes in vitro through a pathway which involves the P2X7 receptor (P2X7R), p38 MAPK cascade, and lysosomal acid sphingomyelinase (A-SMase) [15]. As such, P2X7R antagonists and inhibitors of p38 MAPK and A-SMase can regulate MV shedding and IL-1 β release from glial cells. FTY720 (Gilenya), an immunomodulator drug marketed as the first oral sphingosine-1-phosphate receptor modulator for treatment of multiple sclerosis, also inhibits lysosomal A-SMase [16].

The aim of this study was to study the roles of extracellular ATP via the P2X7R-p38 MAPK-A-SMase pathway in secondary injury after TBI. In this study, P2X7R was detected predominately in microglia of the cerebral cortex. After TBI, the microglia transformed into the amoeba-like form, shedding many MV-like particles at the injured and adjacent regions. The P2X7R antagonist, A804598, and FTY720 reduced significantly the number of MV-like particles in the injured/adjacent regions and in cerebrospinal fluid (CSF) and improved the outcomes of TBI. These data indicate that MV-like particles discharged by microglia after TBI may be involved in the development of local inflammation and secondary nerve cell injury.

Material and methods

Animals and surgical procedures

Male Sprague–Dawley rats weighing 250–300 g were provided by the Animal Center of Second Military Medical University. All experimental procedures were approved by the Institutional Animal Care and Use Committee at Second Military Medical University and conformed to the UK

Animals (Scientific Procedures) Act 1986 and associated guidelines on the ethical use of animals.

Rat TBI model

The rats were anesthetized by an intraperitoneal injection of 10% chloral hydrate, 0.3 ml/100 g. A rectal probe was inserted and the animals were positioned on a thermistor-controlled heating pad. All surgery was done under sterile conditions. The rats were randomly allocated into four groups as follows: a control (sham-operated) group, a TBI group, a group of TBI treated with A804598, and a group of TBI treated with FTY720, each group having 40 rats. The control group underwent craniotomy alone and received no medication. The TBI group underwent craniotomy followed by brain injury and received a physiological saline injection. The TBI group treated with A804598 underwent craniotomy followed by brain injury and then received A804598. The group of TBI treated with FTY720

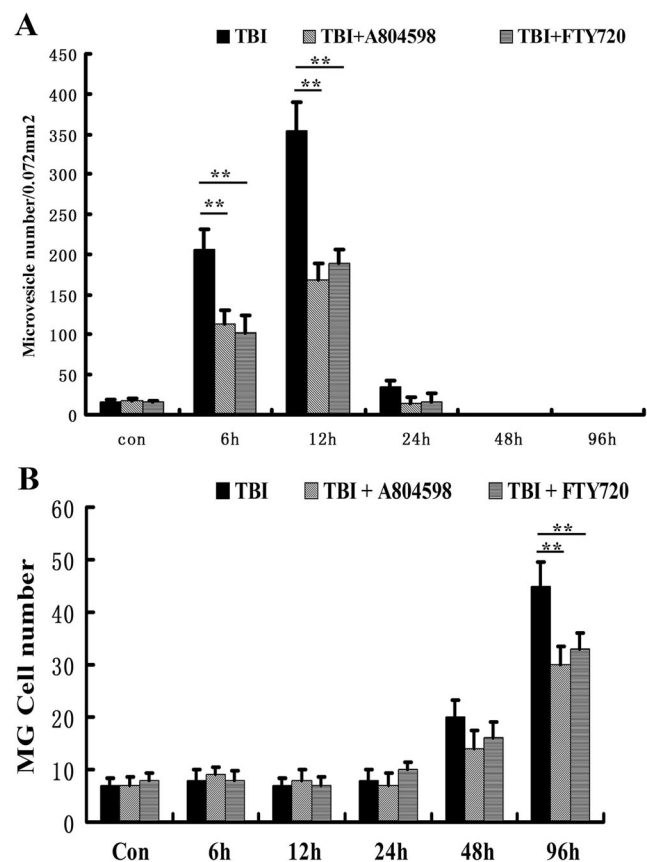


Fig. 2 Quantitative analysis of MV-like particles (a) and microglial cells (b) with P2X7R-ir after TBI. The number of MV-like particles and microglial cells is expressed as mean \pm SEM ($n = 6$). Note that MV-like particles were mainly detected at 6 and 12 h after TBI; both A804598 and FTY720 reduced significantly the number of MV-like particles at 6 and 12 h and the number of microglial cells at 96 h. $**p < 0.01$

underwent craniotomy followed by brain injury and then received FTY720 injection.

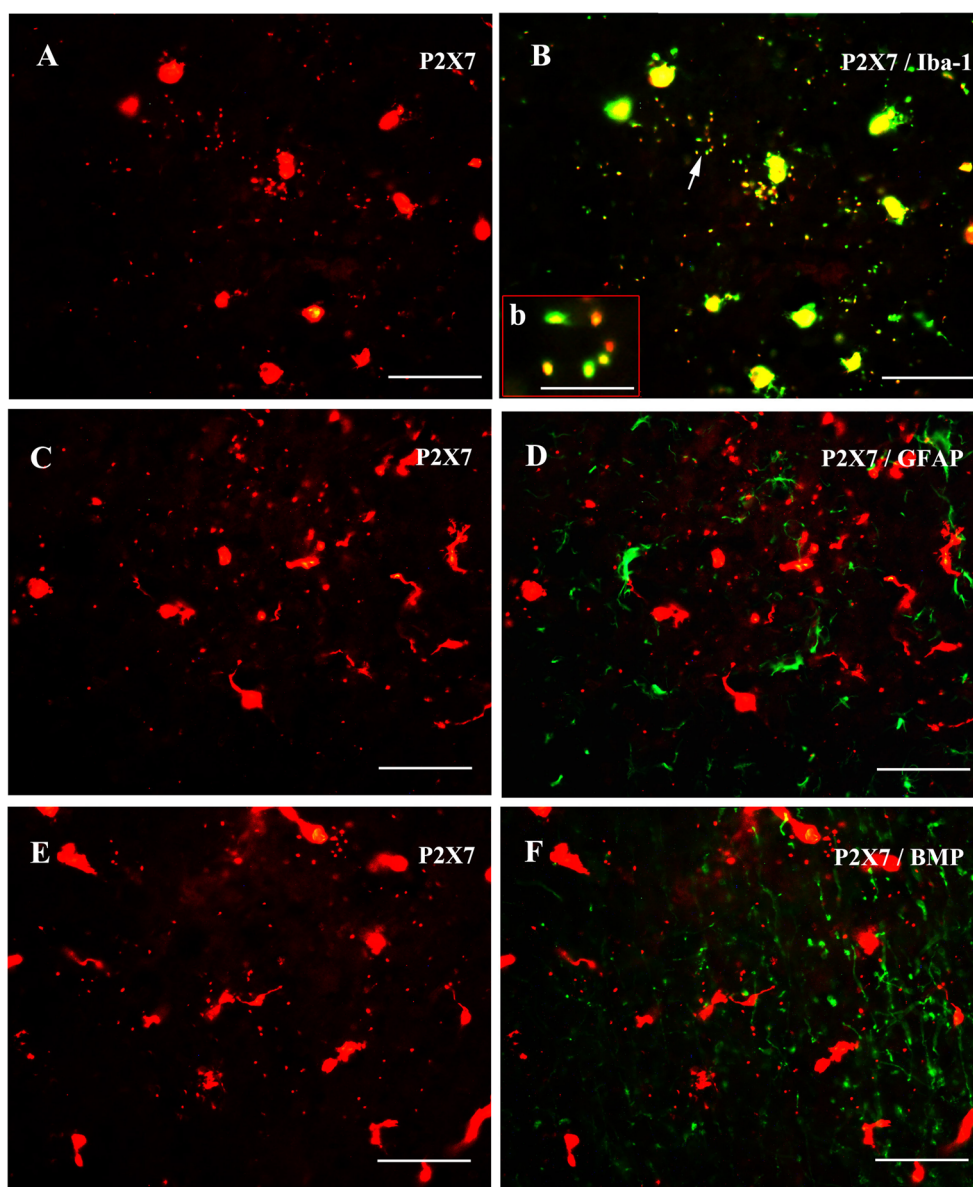
For the production of brain injury, a modified weight drop technique was used according to the protocol of Feeney's [17]. A craniotomy ($6 \times 6 \text{ mm}^2$), centered over the right parietal cortex at bregma -3.5 and 3.5 mm lateral to the midline, was done using a dental drill. A 20-g weight was dropped from a height of 20 cm onto 4.5-mm-diameter piston resting on the exposed dura. The device was constructed to prevent bouncing of the weight thus allowing only a single compression.

The P2X7R antagonist A804598 (Tocris) and FTY720 (Santa Cruz) were prepared freshly by dissolving in 0.9% physiological saline and were administered intraperitoneally immediately after trauma. The dosages of A804598 and FTY720 were 10 and 0.2 mg/kg, respectively, once daily for the continuous 5 days.

Immunohistochemistry

The rats were anesthetized and perfused intracardially with saline, followed by 4% (w/v) paraformaldehyde in 0.1 mol/L PBS, pH 7.4. Brains were removed and fixed overnight in 4% (w/v) paraformaldehyde, then transferred to 25% sucrose in phosphate-buffered saline (PBS) and kept in the solution until they sank to the bottom. Thereafter, the tissue blocks were rapidly frozen and coronal sections ($20 \mu\text{m}$ in thickness) were cut with a Leica cryostat and floated them in PBS. The following protocol was used for immunofluorescence. The sections were washed 3–5 min in PBS and then preincubated in a blocking solution (10% normal bovine serum, 0.2% Triton X-100, 0.4% sodium azide in 0.01 mol/l PBS pH 7.2) for 30 min followed by

Fig. 3 Double immunofluorescence of P2X7R-ir (red), Iba-1 (green), GFAP (green), and MBP (green) in the cerebral cortex of rats 12 h after TBI. **a, c, e** P2X7R-ir. **b, d, f** Merged images of Iba-1-ir, GFAP-ir, and MBP-ir with **a, c, and e**, respectively. **b** Magnified image of the region of **b** indicated by an arrow. Note that almost all the MV-like particles and cells with P2X7-ir are also labeled with Iba-1-ir but not with GFAP-ir or MBP-ir. The scale bars in **a–f** = $60 \mu\text{m}$, **b** = $10 \mu\text{m}$



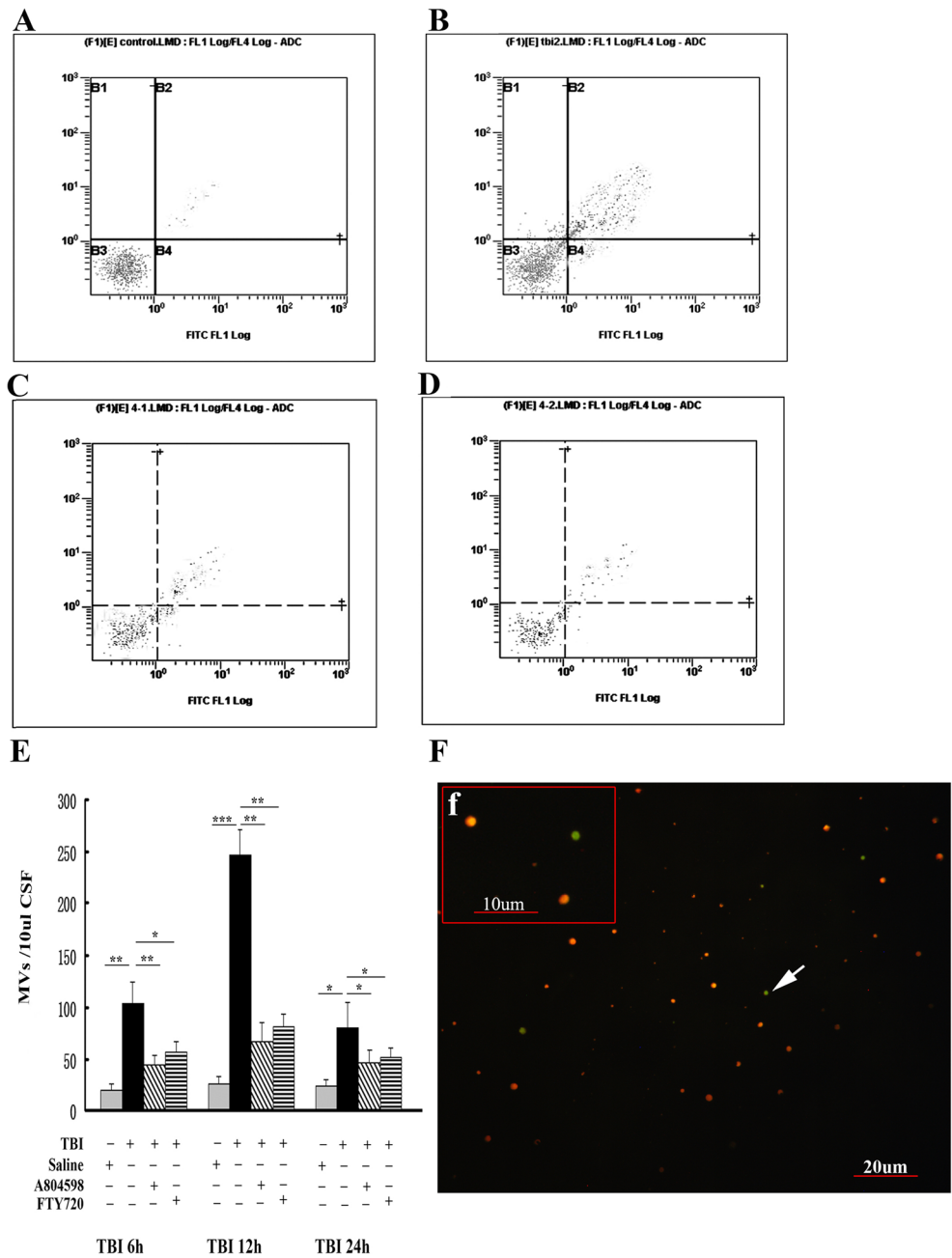
incubation with the primary antibodies (P2X7 (1:1000), Alomone, rabbit polyclonal, APR-004; NeuN (1:500), Millipore, mouse monoclonal, clone A60; Iba-1 (1:500), Abcam, goat polyclonal, ab107159, biotin-conjugated IB4 (1:200), Sigma, L3019; GFAP (1:400), Boster (1:400), mouse monoclonal, BM0055) at room temperature overnight. Subsequently, the sections were incubated with Cy3-conjugated donkey anti-rabbit IgG (Jackson, 711-165-152) diluted 1:400 for P2X7, FITC-conjugated donkey anti-mouse IgG (Jackson, 705-475-151) 1:200 for NeuN and GFAP, FITC-conjugated

donkey anti-goat IgG (Jackson, 715-475-003) 1:200 for Iba-1, and Fluorescein-conjugated streptavidin (Jackson, 016-010-018) 1:200 for IB4. All incubations were separated by 5–10 min washes in PBS.

TUNEL method and double labeling of TUNEL and immunohistochemistry

In situ labeling of DNA fragmentation (terminal deoxynucleotidyl transferase-mediated UTP nick end labeling (TUNEL)) was carried out with an in situ cell

Fig. 4 Flow cytometry and immunocytochemical analysis of MV-like particles in CSF after TBI. **a–d** Results from control, TBI, TBI+A804598, and TBI+FTY720 groups at 12 h after TBI. **e** Summary of flow cytometry of CSF from different groups. Note that the number of MV-like particles reaches a peak at 12 h. Both A804598 and FTY720 significantly reduced the number of MV-like particles at 6 and 12 h. **f** Immunocytochemical analysis of MV-like particles with P2X7R (red) and Iba-1 immunostaining (green). Note that most of MV-like particles with P2X7R-ir are also labeled by Iba-1, although some of them are not. An arrow indicates an MV-like particle with Iba-1 not labeled by P2X7R-ir (shown at higher magnification in **f**)



death detection kit, Fluorescein (Roche, Mannheim, Germany, catalog number 11684795910), according to the manufacturer's instructions. The apoptotic cells were labeled with green fluorescence.

After detection of TUNEL, the sections were washed 3–5 min in PBS and then preincubated in a blocking solution for 30 min followed by incubation with the primary antibodies (NeuN (1:500), Millipore, mouse monoclonal, clone A60; Iba-1 (1:500), Abcam, goat polyclonal, ab107159, mouse monoclonal GFAP (1:400), Boster, mouse monoclonal MBP (1:400), Boster and olig2, Millipore, rabbit polyclonal, ab9610) at room temperature overnight. Subsequently, the sections were incubated with Cy3-conjugated donkey anti-rabbit IgG (Jackson, 711-165-152) diluted 1:400 for Olig2, Cy3-conjugated donkey anti-mouse IgG (Jackson, 715-165-150) 1:400 for NeuN and GFAP, and Cy3-conjugated donkey anti-goat IgG (Jackson, 705-165-147) 1:400 for Iba-1. All incubations were separated by 5–10 min washes in PBS.

Flow cytometry

Rats were anesthetized by intraperitoneal injection with 4% chloral hydrate; CSF was sampled from the cisterna magna using a glass capillary and checked for the absence of blood contamination. CSF pooled from three rats was diluted with ice-cold PBS and subjected to differential centrifugation to obtain microvesicles at $16,000\times g$ for 1 h. The resulting pellets were resuspended in $1\times$ binding buffer (0.01 M HEPES/NaOH (pH 7.4), 0.14 M NaCl, 2.5 mM CaCl_2) and were then stained using the Annexin V-FITC/PI detection kit. The labeled samples were analyzed by flow cytometry (BD Biosciences, San Jose, CA, USA).

Photomicroscopy

Images were taken with a Nikon digital camera DXM1200 (Nikon, Japan) attached to a Nikon Eclipse E600 microscope (Nikon). Images were imported into a graphics package (Adobe Photoshop 5.0, USA).

Western blot

For Western blotting, the rats were killed after 6 h, 12 h, 24 h, 48 h, 4 days, and 7 days of TBI. The injured/adjacent cerebral cortexes and contralateral cortexes were removed immediately and lysed with 20 mM Tris-HCl buffer, pH 8.0, containing 1% Nonidet P 40, 150 mM NaCl, 1 mM EDTA, 10% glycerol, 0.1% L-mercaptoethanol, 0.5 mM dithiothreitol, and a mixture of proteinase and phosphatase inhibitors (Sigma). Protein concentration was determined by the BCA protein assay method using bovine serum albumin (BSA) as standard. One hundred

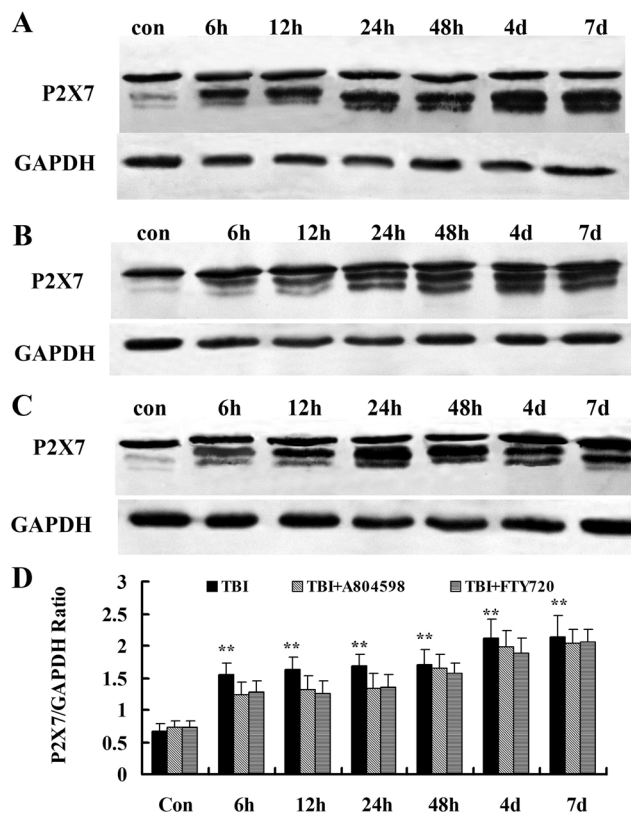
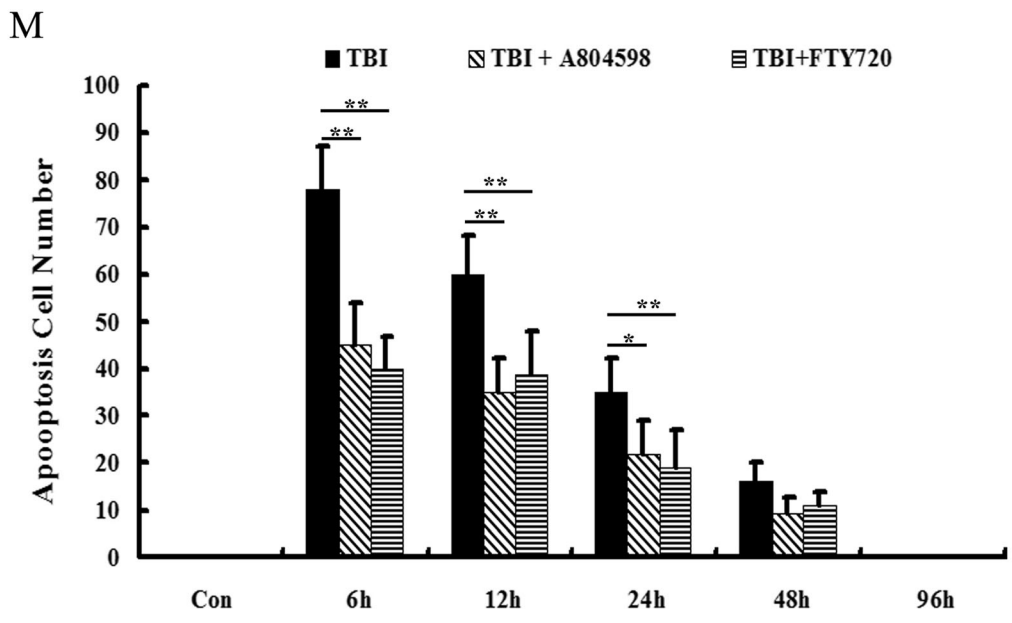
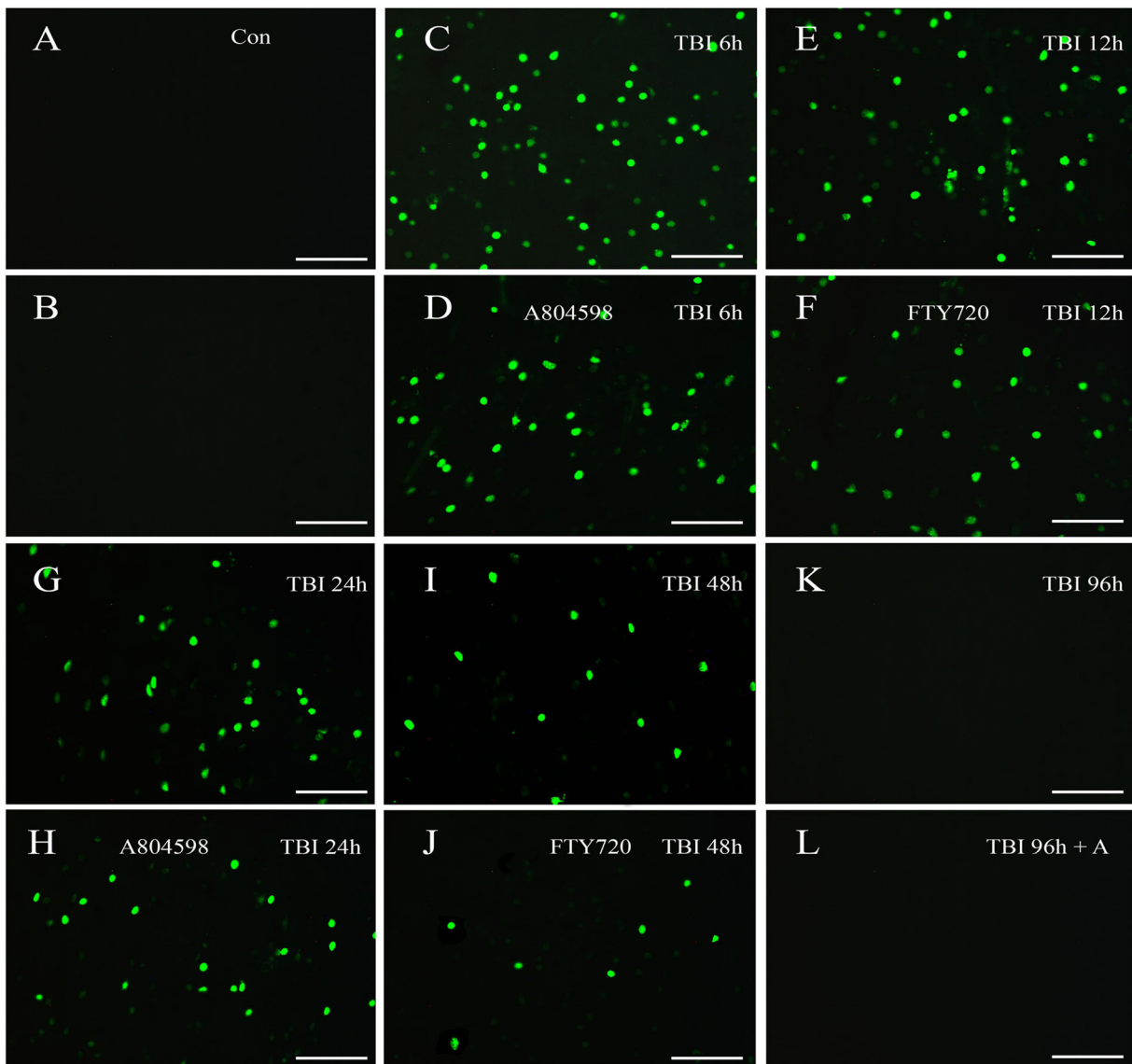


Fig. 5 Expression of P2X7R detected by Western blotting in the cerebral cortex from TBI (a), TBI+A804598 (b), and TBI+FTY720 (c) groups. **d** Summary of P2X7R/GAPDH ratio. Data are representative of five rats per group. The ratio of P2X7R/GAPDH was analyzed with one-way ANOVA followed by Dunnett's post hoc test (** $p < 0.01$ vs. control sham-operated rats). The results show that expression of P2X7R protein increased significantly from 6 h to 7 days after TBI but was not affected by A804598 or FTY720

micrograms of protein samples was loaded per lane, separated by SDS-PAGE (10% polyacrylamide gels), and then was electrotransferred onto nitrocellulose membranes. The membranes were blocked with 10% non-fat dry milk in Tris-buffered saline for 1 h and incubated overnight at 4 °C with P2X7 (1:1000, Alomone, rabbit polyclonal), p-p38(1:1000, CST, rabbit polyclonal), tubulin (1:1000, Beyotime, mouse monoclonal), and GAPDH (1:1000, Beyotime, mouse monoclonal) diluted in 2% BSA in PBS. The membranes were then incubated with alkaline phosphatase-conjugated goat anti-

Fig. 6 Effect of A804598 and FTY720 on cell apoptosis in the cerebral cortex after TBI. **a, c, e, g, i, k** TUNEL staining from the control, 6, 12, 24, 48, and 96 h groups, respectively. **d, h, l, f, j** TUNEL staining from TBI+A804598 and TBI+FTY720. **M** is the summary of the number of TUNEL-positive cells in the different groups. Note that A804598 or FTY720 treatment significantly reduced the number of apoptotic cells. Values are expressed as the mean \pm SEM. ** $p < 0.01$ TBI+A804598 groups or TBI+FTY720 groups versus saline-treated groups. All the scale bars = 60 μm



rabbit IgG (Sigma) or goat anti-mouse IgG (Sigma) diluted 1:5000 in 2% BSA in PBS for 1 h at room temperature. The color development was performed with 400 µg/ml nitro-blue tetrazolium, 200 µg/ml 5-bromo-4-chloro-3-indolyl phosphate, and 100 mg/ml levamisole in TSM2 (0.1 mol/l Tris-HCl buffer, pH 9.5, 0.1 mol/l NaCl, and 0.05 mol/l MgCl₂) in the dark. Bands were scanned using a densitometer (GS-700; Bio-Rad Laboratories)

ELISA for tissue IL-1β levels

Protein samples from the different groups of rats were collected as for the Western blot protocol described above. The samples were stored at -20 °C until analyzed for IL-1β using the rat IL-1β ELISA kit from Multisciences. Assays were carried out according to the manufacturer's instructions and the optical density (O.D.) was read at 450 nm using a Bio-Rad Model 680 Microplate Reader within 15 min. The standard curve was used to determine the amount of protein in the samples from the different groups of rats. IL-1β levels in the rat cerebral cortex tissue were expressed as picograms per milligram of protein sample.

Morris water maze

At 8 days, spatial learning and memory were tested with the Morris water maze [18] which was a circular black tank of 130 cm in diameter and 60 cm in height. The tank was filled to a depth of 30 cm water at 25 ± 1 °C. The maze was divided into four equal quadrants. The trials were performed according to Vorhees' method [19].

Spatial acquisition All rats received a training trial consisting of daily sessions of four consecutive trials for 5 days. The hidden platform (diameter 10 cm, 1.5 cm below the water surface) was positioned in the middle of the southwest (SW) quadrant for all rats. The rats were released into the tank facing the maze wall at north (N), west (W), south (S), or east (E) quadrants in a predetermined pseudorandom order. A trial was terminated as soon as the rat found the platform; if the rat did not succeed within 120 s, it was guided onto the platform with a stick. The rat was allowed to stay on the platform for 20 s before being removed.

Probe trial Immediately after the final training trial, the platform was removed. Rats were released into the pool at the NE position and allowed to swim freely for 2 min. The time needed to find the platform (escape latency) in the training trials and time spent in the SW quadrant in the probe trial were recorded. The mean value of four escape latencies in the daily four training trials was taken as the escape latency for the

rat. Values from eight rats in the same group were averaged to generate a mean escape latency for that day.

Quantitative analysis

Neuronal damage, apoptosis, and MV-like particles were quantified by counting the number of surviving neurons, positive neurons for TUNEL, and MV-like particles with P2X7-ir (< 2.0 µm) in the images at high magnification (×400) from the injured and adjacent regions. The numbers of surviving/TUNEL-positive neurons and total neurons in the regions were counted and analyzed by NIS-Elements D3.1 system (Nikon, Japan). Ten sections were used for each rat and the mean number of these ten sections was calculated. Six rats were used for each experimental group.

To quantify glial activation, we measured the value of the average area optical density (AAOD) for immunohistochemistry images from the injured region stained with antibodies against GFAP using NIS-Elements D3.1 system (Nikon, Japan). Pictures were taken using the same method as mentioned above. Ten images (×200) were randomly selected for each animal, and the mean AAOD of these ten fields was considered as the AAOD of the animal.

Statistical analysis

Results are expressed as mean ± SEM (*n* = 5–6). Values were analyzed using a one-way analysis of variance (ANOVA) followed by Dunnett's post hoc test. *P* < 0.05 was considered to be statistically significant.

Results

The number of TBI-induced microglial MV-like particles in the cerebral cortex after TBI were reduced by a P2X7R antagonist and the immune modulator FTY720

In the normal conditions, P2X7R immunoreactivity (P2X7R-ir) was detected only in the cells that were also labeled with Iba-1 (a microglial marker) antibody (Fig. 1a, d). This result implied that the P2X7R is predominately expressed in microglial cells in the cerebral cortex of adult rats. After TBI, the microglial cells with P2X7R-ir transformed into amoeboid-like cells in the injured and adjacent regions. There were numerous MV-like particles with P2X7R-ir around the amoeboid cells, and the number of these particles reached a peak at 12 h after TBI and disappeared after 48 h (Figs. 1b, c, g, h and 2a). The number of amoeboid-like cells with P2X7R-ir increased 48 h after TBI (Figs. 1 and 2). A804598 and FTY720 inhibited significantly the number of MV-like particles and amoeboid-like cells with P2X7R-ir (Figs. 1e–l and 2b). In order to analyze the source of

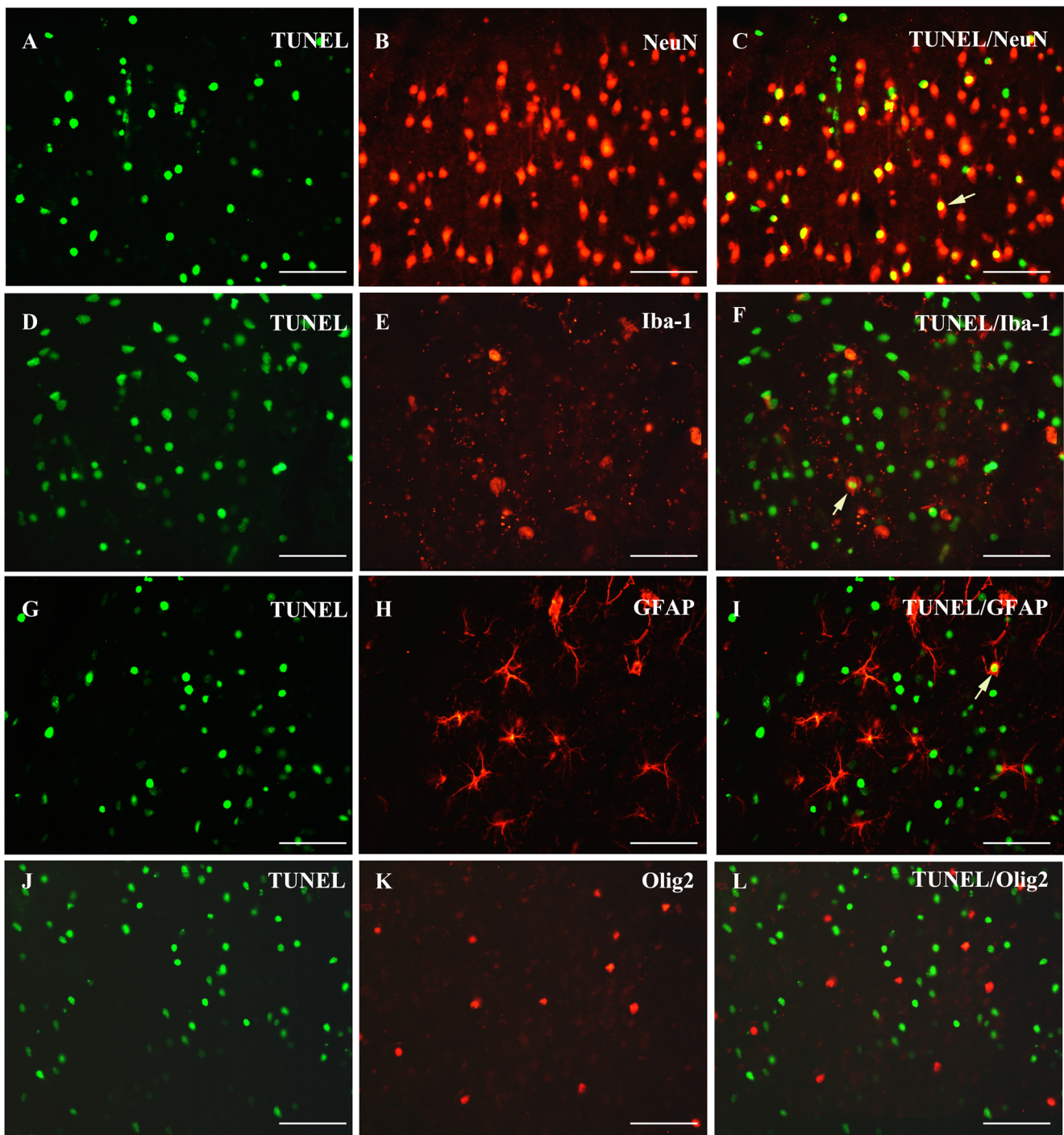


Fig. 7 Cell type analysis of apoptotic cells in the cerebral cortex at 6 h after TBI. **a, d, g, j** TUNEL-positive cells. **b, e, h, k** NeuN-positive, GFAP-positive, Iba-1-positive, and Olig2-positive cells in the same fields of **a, d, g, and j**, respectively. **c, f, i, l** Immerged images from **a** and **b, d**

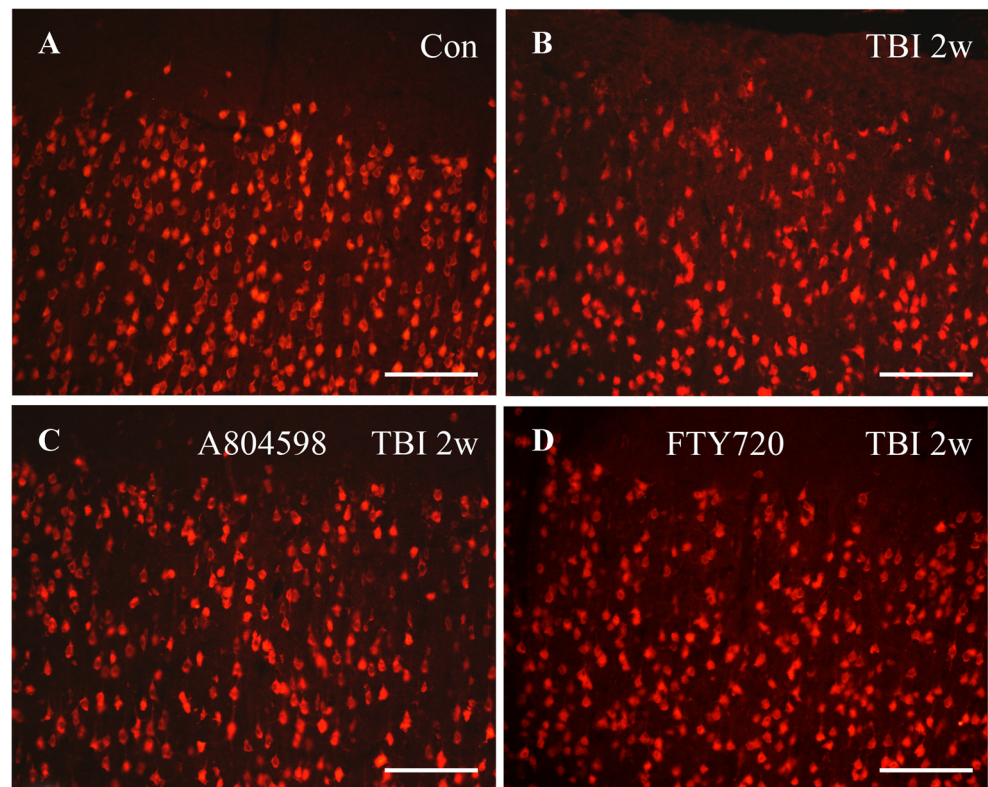
and **e, g** and **h**, and **j** and **k**. Note that most of the apoptotic cells were NeuN-positive, occasionally Iba-1- or GFAP-positive, but never Olig2-positive. The results indicate that most of the apoptotic cells after TBI are neurons. All scale bars = 60 μ m

the MV-like particles, a double immunofluorescence technique was carried out. The results showed that almost all the MV-like particles were also labeled with Iba-1 but not with GFAP or MBP (Fig. 3). The results

confirmed that these MV-like particles predominately originated from microglial cells.

CSF samples were collected from TBI, TBI+A804598, and TBI+FTY720 group rats and analyzed by flow cytometry. The

Fig. 8 Effect of A804598 and FTY720 on neuronal survival rate in the cerebral cortex after TBI. **a–d** NeuN immunostaining from the control group, TBI group, TBI+ A804598 group, and TBI+ FTY720 group 14 days after TBI, respectively. **e** Summaries of the number of survival neurons. Note that both A804598 and FTY720 treatment increased significantly the number of surviving neurons. Values are expressed as mean \pm SEM. * $p < 0.05$, ** $p < 0.01$. 2w (2 weeks) = 14 days. All scale bars = 60 μ m



results showed that the number of particles with Annexin V-FITC reached a peak value 12 h after TBI. A804598 and FTY720 inhibited significantly the number of particles with Annexin V-FITC (Fig. 4). The particles were further analyzed by immunocytochemistry. The results showed that 85% of the particles were both P2X7R-ir and Iba1-ir (Fig. 4f), which implies that most of the particles in the CSF samples originated from microglial cells.

Western blot analysis showed that expression of P2X7R protein in the injured areas and adjacent cerebral cortex increased gradually after TBI (Fig. 5). A804598 and FTY720 did not inhibit P2X7R protein expression significantly, as shown in Fig. 5. The molecular weight of the three bands with

P2X7R-ir was located around 72 kd. The bands disappeared after the antibody was preincubated with the control peptide antigen (supplementary Fig. 1).

The number of apoptotic cells was reduced and the number of neurons that survived was increased in the cerebral cortex after TBI by use of a P2X7R antagonist and the immune modulator FTY720

Apoptotic cells were studied using the TUNEL technique. The results showed that many apoptotic cells were detected from 6 to 48 h after TBI. A804598 and FTY720 decreased significantly the number of the apoptotic cells, as shown in Fig. 6.

The double labeling technique of TUNEL and immunohistochemistry showed that most of the apoptotic cells were NeuN-positive, occasionally Iba-1- or GFAP-positive, but never Olig2-positive (Fig. 7). The result indicates that most of the apoptotic cells are neurons after TBI.

The neurons that survived were studied by NeuN immunostaining. The results showed that the number of NeuN-positive neurons decrease significantly in the TBI group, compared to the control group. Both A804598 and FTY720 increased the survival of neurons in the injured and adjacent regions (Fig. 8). These results show that A804598 and FTY720 have neuroprotective roles after TBI.

P2X7R or FTY720 mediates IL-1 β expression after TBI

IL-1 β expression was detected at a low level in the sham rat cerebral cortex. After TBI, the level of expression of IL-1 β increased. Forty-eight hours after TBI, the level of expression of IL1 β reached a peak. Treatment with A804598 or FTY720 significantly reduced the expression of IL-1 β within the cerebral cortex, as assessed by ELISA (Fig. 9).

The p38 signaling pathway has been shown to be involved in MV shedding and IL-1 β secretion from microglia. Phosphorylated p38 was detected in the sham rat cerebral cortex at a low level. After TBI, the level of phosphorylated p38 increased. At 12 h after TBI, the level of phosphorylated p38 reached a peak (Fig. 10). Treatment with A804598 or FTY720 significantly reduced the level of phosphorylated p38 at 12 and 24 h, as assessed by Western blotting (Fig. 10).

Inhibition of the P2X7R FTY720 reduces TBI-induced glial activation

Reactive astrogliosis was assessed by immunohistochemical analysis of the expression of GFAP (an

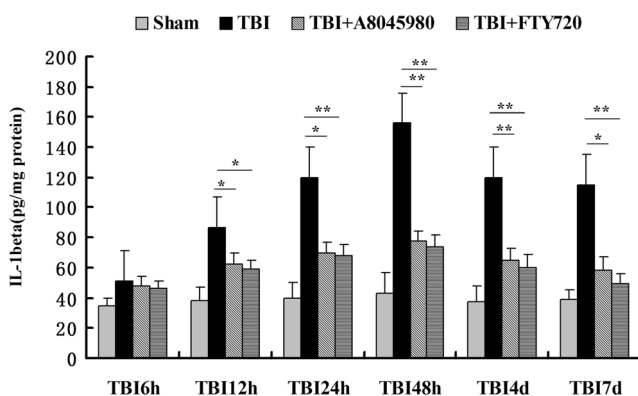


Fig. 9 Effect of A804598 and FTY720 on expression of interleukin (IL)-1 β in the cerebral cortex after TBI. IL-1 β was detected by ELISA. Both A804598 and FTY720 reduced significantly the levels of IL-1 β . Data are expressed as mean \pm SEM. * p < 0.05, ** p < 0.01

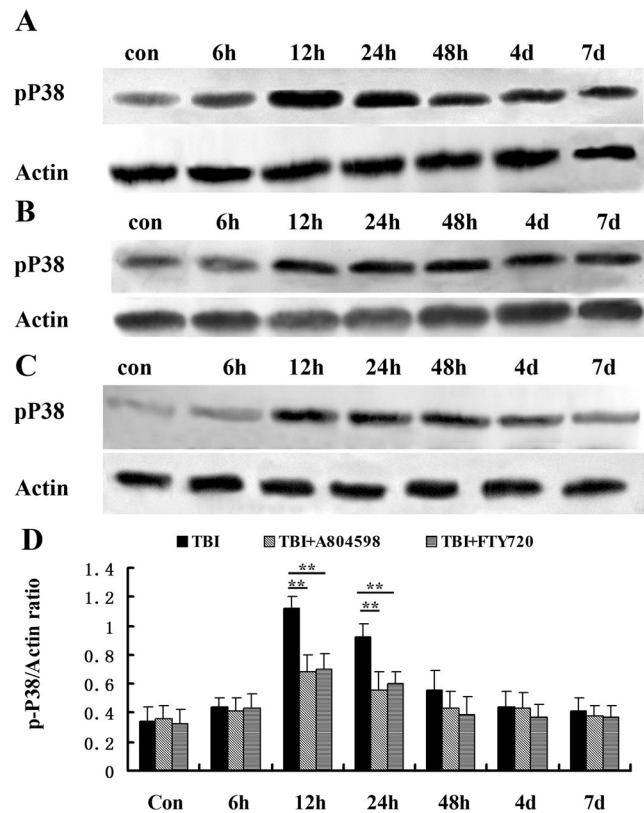
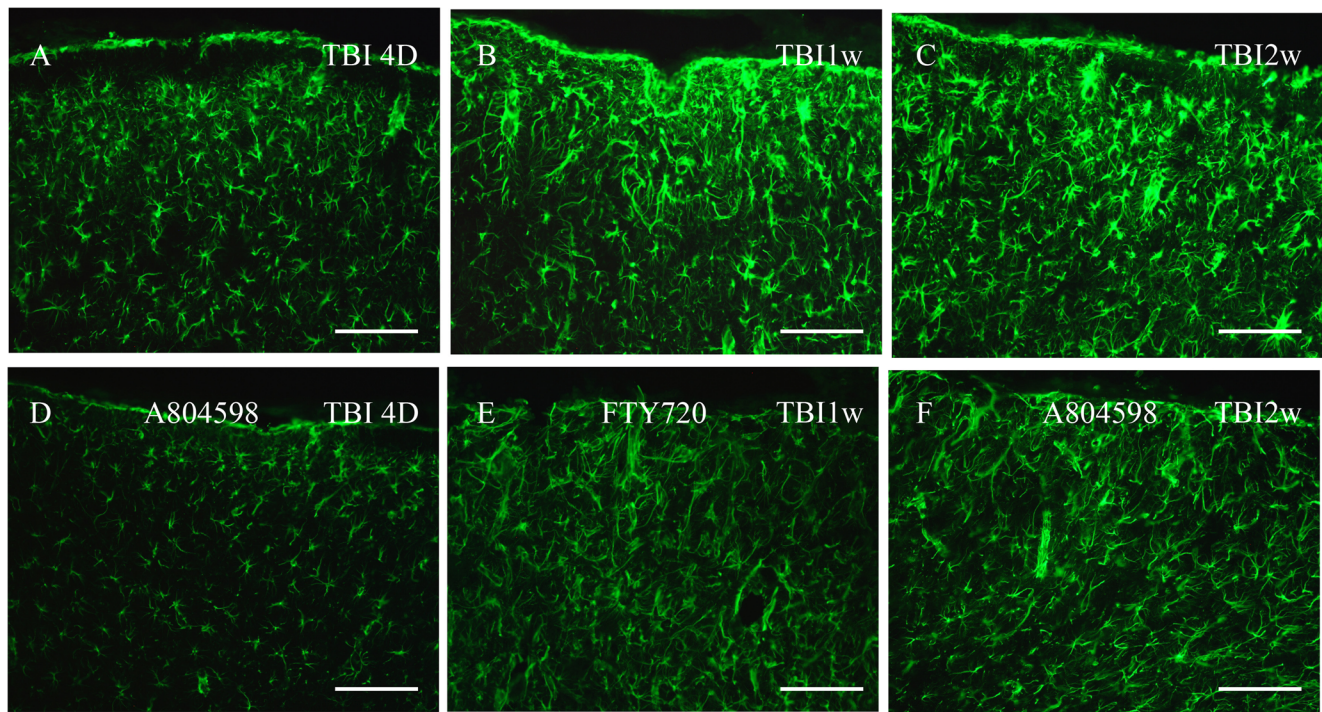


Fig. 10 Expression of phosphorylation P38 (pP38) detected by Western blotting in the cerebral cortex from TBI (a), TBI+A804598 (b), and TBI+FTY720 (c) groups. **d** Summary of pP38/actin ratio. Data are representative of five rats per group. The ratio of pP38/actin was analyzed with one-way ANOVA followed by Dunnett's post hoc test (** p < 0.01 TBI vs. TBI+A804598 or TBI+FTY720 rats). Statistical analysis shows that pP38 protein increased significantly at 12 and 24 h after TBI, which was inhibited by A804598 or FTY720, significantly

astrocyte marker) in the injured and adjacent regions of cerebral cortex at 12 h, 2 days, 4 days, 7 days, and 14 days after TBI. The scattered GFAP-ir cells with thin and long processes were detected in the cerebral cortex region of the sham rat. However, both the immunostaining density and the number of GFAP-ir cells significantly increased in the saline group. Treatment with A804598 or FTY720 markedly attenuated the increase of immunostaining density and the number of GFAP-ir cells when compared to the saline group (Fig. 11).

Inhibition of the P2X7R or FTY720 improves neurobehavioral outcomes after TBI

Spatial memory was evaluated using the Morris water maze. During the 5-day hidden platform trial, escape latency of sham and the three experimental groups decreased in a day-dependent pattern. However, the sham group took significantly less time to find the platform than the saline group on all 5 days.



G

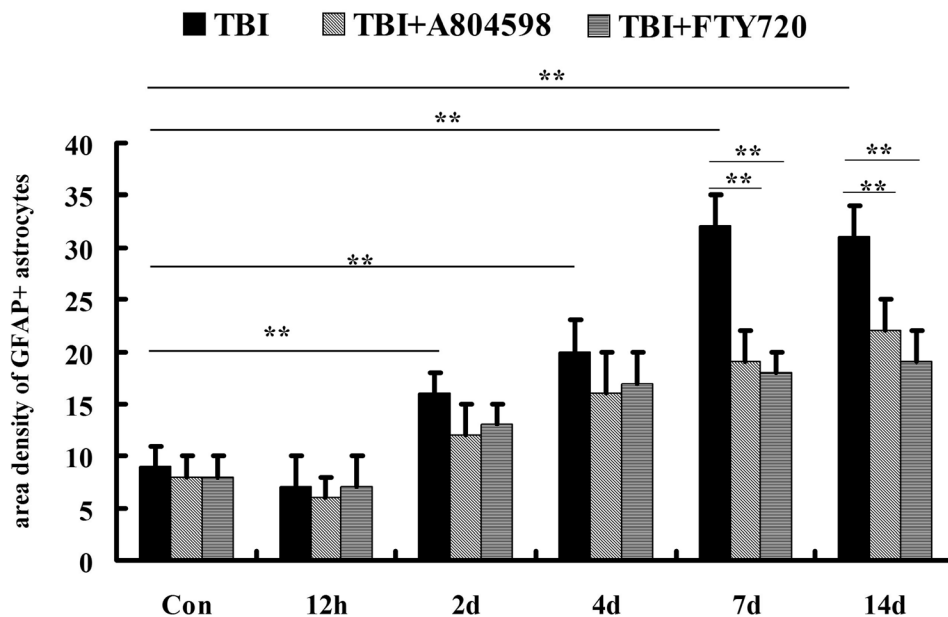


Fig. 11 Effect of A804598 and FTY720 on astrogliosis in the cerebral cortex after TBI. **a–f** Astrocytes with GFAP-ir at 4 days, 7 days (1w), and 14 days (2w) in the TBI+saline groups (**a–c**), TBI+A804598 groups (**d**, **f**), and TBI+FTY720 group (**e**) respectively. **g** Quantitative analysis of average area optical density (AAOD) of astrocytes with GFAP-ir. Data are

expressed as mean \pm SEM ($n = 6$). $**p < 0.01$. Statistical analysis shows that density of GFAP-ir increased gradually after TBI. A804598 or FTY720 reduced the density of GFAP-ir significantly at 7 and 14 days after TBI

In addition, the saline group required significantly more time to find the platform than the A804598 and FTY720 groups after the ninth day. In the probe trial, the saline group spent significantly less time than the other three groups in the SW quadrant. There was no significant difference among the sham, A804598, and FTY720 groups (Fig. 12).

Discussion

The main finding of this study is that the P2X7R antagonist A804598 and the immune modulator FTY720 reduced neuron apoptotic cell death and increased the survival of neurons in the injured cerebral cortex injured and adjacent regions after

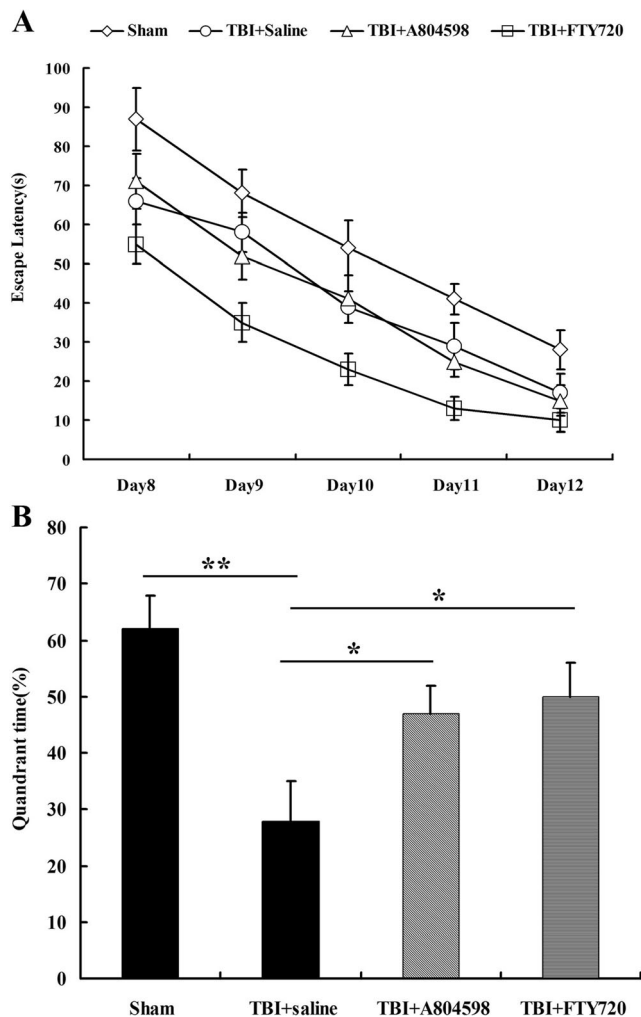


Fig. 12 Effect of A804598 and FTY720 on spatial learning and memory in the water maze. **a** Escape latency to find the platform during the 5 days of the training trial from the 8th to the 12th day after TBI. **b** Time spent during the probe trial in the quadrant where the platform had been located. Values are expressed as mean \pm SEM. $**p < 0.01$, $*p < 0.05$. Statistical analysis shows that spatial learning and memory were affected significantly by TBI. Both A804598 and FTY720 improved spatial learning and memory after TBI

TBI. P2X7R expression was up-regulated on microglial cells after TBI. Inhibition of the P2X7R and FTY720 reduced TBI-induced microglial MV-like particles, IL-1 β expression, P38 phosphorylation, glial activation in the cerebral cortex, and improved neurobehavioral outcomes after TBI.

ATP is an important signaling molecule mediating interactions among various cell types in the brain [10–12, 20–26]. A low level of extracellular ATP is maintained in physiological conditions [25, 27], with the cytoplasmic ATP concentration is in the millimolar range. Activated immune cells [28], macrophages [29], microglia [30], astrocytes [31], platelets [32], and dying cells [33] may release high concentrations of ATP into the extracellular space. Massive release of ATP also occurs after metabolic stress and trauma, and high levels of ATP persist in the injured zone for an extended time [8, 20,

34–36]. ATP is not rapidly degraded during inflammation or oxidative stress conditions, as the enzymes for extracellular ATP degradation are inhibited [37].

The receptors for extracellular ATP are termed P2 receptors, which have been divided into P2X and P2Y receptors on the basis of pharmacology and molecular cloning. Currently, seven subtypes of ionotropic P2X receptors (non-selective cation channels) and eight subtypes of metabotropic P2Y receptors (G protein-coupled receptors) have been characterized [38, 39]. The P2X7R is predominantly expressed on microglia and ependyma of the CNS [40, 41]. P2X7R can be activated by high concentrations of ATP. Sustained stimulation of P2X7R on microglia leads to the activation of microglia, which produces reactive oxygen species and pro-inflammatory cytokines and is involved in neuroinflammation in many CNS diseases including, Alzheimer's disease [42], epilepsy [43], spinal cord injury [8, 44], multiple sclerosis (MS) [45], and traumatic brain injury [46].

Our previous data and other researchers have shown that high concentrations of extracellular ATP can stimulate microglial cells or macrophages to shed MVs [47–49]. MVs belong to the group of extracellular vesicles (EVs). Increasing evidence has shown that EVs play important roles in intercellular communications by serving as vehicles for transfer between cells of membrane and cytosolic proteins, lipids, and RNA. Those originating from endosomal membrane are called exosomes, and those originating from plasma membrane are called MVs [50].

The present data has shown that MV-like particles from the microglial cells were mainly detected during a short time period of 6–12 h, and dramatically decreased at 24 h, disappearing from 48 h after TBI. The appearance and disappearance of these MV-like particles were accompanied by morphological changes of the microglial cells, as they ramified to amoeboid microglia. These data imply that MV-like particles are released during the processes of microglial morphological change. Increasing data has shown that purinoceptors are involved in the morphological changes of microglia [21, 27, 51] and MV shedding [13, 47–49]. Persistently high ATP release was also detected in the peritraumatic region during the early stage of 2–6 h and returned to the background level 24 h after spinal cord injury [8]. The time course of the ATP concentration change was similar to that of shedding of the MV-like particles detected in this study. Thus, high ATP release might be expected to be evident during the early stages, 6–12 h after TBI. These high concentrations of ATP may be involved in the MV-like particle shedding and morphological changes of microglial cells, although further experiments are needed to answer this issue.

Increasing evidence has shown that MVs discharged by activated microglia act as amplifying agents of inflammation and has identified MVs as a marker and therapeutic target of brain inflammation [13]. P2X7R-induced MV shedding acts as a secretory pathway for rapid release of IL-1 β and may

represent a general mechanism for secretion of leaderless secretory proteins from P2X7R-expressing myeloid cells [13, 47, 52]. P2X7R, P38 MAPK, and A-SMase play key roles in MV shedding from microglia [13].

A report showed that mice, where microglia were p38-deficient (p38 KO), were protected against TBI-induced motor deficits and synaptic protein loss. In wild-type (WT) mice, TBI produced microglia morphological activation that lasted for at least 7 days; however, p38 KO mice failed to activate this response. The results showed that the p38 signaling pathway in microglia could be contributing to the secondary neuroinjury after TBI [53]. In this study, we also showed that phosphorylation levels of P38 protein increased after TBI. Both A804598 and FTY720 decreased this level. This result further confirmed that the P38 pathway plays a role in secondary neuroinjury after TBI.

FTY720 (Gilenya) is an analog of the naturally occurring myriocin. The therapeutic action of FTY720 in MS is to inhibit the exit of autoreactive memory T cells from secondary lymphoid organs to produce a peripheral lymphopenia [54]. FTY720 has been marketed as the first oral sphingosine-1-phosphate receptor modulator for the treatment of MS, but it also inhibits lysosomal A-SMase [16].

The present data has shown that both A804598 and FTY720 significantly decreased the number of MV-like particles in the injured/adjacent cerebral cortex regions and CSF after TBI and improved the outcomes of neuronal survival, gliosis, and neurobehaviour after TBI. These data imply that A804598 and FTY720 could be used as drugs for treatment of secondary neuronal injury after TBI, as they target P2X7R and A-SMase, respectively. We believe that P2X7R and A-SMase could be used as new therapeutic targets for TBI.

Astrogliosis is the hypertrophy and increase in number of astrocytes due to the destruction of nearby neurons from different pathological causes, which alters astrocyte activities, both through gain and loss of functions that can impact both beneficially and detrimentally on surrounding neural and non-neural cells [55, 56].

Astrogliosis is a ubiquitous but poorly understood hallmark of all CNS pathologies [56]. Many different molecules are found to be able to trigger reactive astrogliosis processes. These astrogliosis molecular mediators can be released by any cell type in the CNS. These mediator molecules include cytokines and growth factors, mediators of innate immunity, neurotransmitters and modulators, small molecules released following cell injury, molecules of oxidative stress, and systemic metabolic toxicity. These molecules, via different signaling routes, trigger different molecular, morphological, and functional changes in reactive astrocytes [56].

IL-1 is an astrogliosis molecular mediator [57, 58]. IL-1 β induces IL-6 release, which further induces astrogliosis [58]. In this study, the data showed that IL-1 β increased after TBI, which was partially blocked by both the P2X7R antagonist,

A804598, and the immune modulator, FTY720. Astrogliosis was also partially inhibited by these two drugs.

In summary, the techniques of immunohistochemistry, TUNEL, Western blotting, flow cytometry, ELISA, and neurobehavioural tests used in this study have shown that the P2X7R antagonist A804598 and the immune modulator FTY720 reduced neuron apoptotic cell death and increased the survival of neurons in the injured cerebral cortex and adjacent regions after TBI. A possible mechanism is that high concentrations of extracellular ATP after TBI, via P2X7R, activate microglial cells, which discharge MV-like particles involving local neuroinflammation. Inhibition of the P2X7R and A-SMase reduced TBI-induced microglial MV-like particles, IL-1 β expression, P38 phosphorylation, and glial activation in the cerebral cortex and improved neurobehavioral outcomes after TBI.

Acknowledgements This work was supported by the National Natural Science Foundation of the People's Republic of China (81471260 to Z. Xiang) and by the Qingnian Science Foundation of Changzheng Hospital, Shanghai, People's Republic of China (2016CZQN05 to R. Ji).

Compliance with ethical standards

Conflicts of interest Xiaofeng Liu declares that she has no conflict of interest.

Zhengqing Zhao declares that she has no conflict of interest.

Ruihua Ji declares that she has no conflict of interest.

Jiao Zhu declares that she has no conflict of interest.

Qian-Qian Sui declares that she has no conflict of interest.

Gillian E. Knight declares that she has no conflict of interest.

Geoffrey Burnstock declares that he has no conflict of interest.

Cheng He declares that she has no conflict of interest.

Hongbin Yuan declares that she has no conflict of interest.

Zhenghua Xiang declares that she has no conflict of interest.

Ethical approval All experimental procedures were approved by the Institutional Animal Care and Use Committee at Second Military Medical University and conformed to the UK Animals (Scientific Procedures) Act 1986 and associated guidelines on the ethical use of animals.

References

- Jennett B (1996) Epidemiology of head injury. *J Neurol Neurosurg Psychiatry* 60(4):362–369
- Langlois JA, Rutland-Brown W, Wald MM (2006) The epidemiology and impact of traumatic brain injury: a brief overview. *J Head Trauma Rehabil* 21(5):375–378
- Davis AE (2000) Mechanisms of traumatic brain injury: biomechanical, structural and cellular considerations. *Crit Care Nurs Q* 23(3):1–13
- Gaetz M (2004) The neurophysiology of brain injury. *Clin Neurophysiol* 115(1):4–18
- Cernak I (2005) Animal models of head trauma. *NeuroRx* 2(3):410–422
- Bramlett HM, Dietrich WD (2007) Progressive damage after brain and spinal cord injury: pathomechanisms and treatment strategies. *Prog Brain Res* 161:125–141

7. Cornelius C, Crupi R, Calabrese V, Graziano A, Milone P, Pennisi G et al (2013) Traumatic brain injury: oxidative stress and neuroprotection. *Antioxid Redox Signal* 19(8):836–853
8. Wang X, Arcuino G, Takano T, Lin J, Peng WG, Wan P et al (2004) P2X7 receptor inhibition improves recovery after spinal cord injury. *Nat Med* 10(8):821–827
9. Kimbler DE, Shields J, Yanasak N, Vender JR, Dhandapani KM (2012) Activation of P2X7 promotes cerebral edema and neurological injury after traumatic brain injury in mice. *PLoS One* 7(7):e41229
10. Franke H, Grummich B, Hartig W, Grosche J, Regenthal R, Edwards RH et al (2006) Changes in purinergic signaling after cerebral injury—involve ment of glutamatergic mechanisms? *Int J Dev Neurosci* 24(2–3):123–132
11. Franke H, Schepper C, Illes P, Krugel U (2007) Involvement of P2X and P2Y receptors in microglial activation in vivo. *Purinergic Signal* 3(4):435–445
12. Abbracchio MP, Verderio C (2006) Pathophysiological roles of P2 receptors in glial cells. *Novartis Found Symp* 276:91–103 discussion 12, 275–81
13. Turola E, Furlan R, Bianco F, Matteoli M, Verderio C (2012) Microglial microvesicle secretion and intercellular signaling. *Front Physiol* 3:149
14. Sadallah S, Eken C, Schifferli JA (2011) Ectosomes as modulators of inflammation and immunity. *Clin Exp Immunol* 163(1):26–32
15. Bianco F, Pravettoni E, Colombo A, Schenk U, Moller T, Matteoli M (2005) Astrocyte-derived ATP induces vesicle shedding and IL-1 beta release from microglia. *J Immunol* 174(11):7268–7277
16. Dawson G, Qin J (2011) Gilenya (FTY720) inhibits acid sphingomyelinase by a mechanism similar to tricyclic antidepressants. *Biochem Biophys Res Commun* 404(1):321–323
17. Feeny DM, Boyeson MG, Linn RT, Murray HM, Dail WG (1981) Responses to cortical injury: I. Methodology and local effects of contusions in the rat. *Brain Res* 211(1):67–77
18. Morris R (1984) Developments of a water-maze procedure for studying spatial learning in the rat. *J Neurosci Methods* 11(1):47–60
19. Vorhees CV, Williams MT (2006) Morris water maze: procedures for assessing spatial and related forms of learning and memory. *Nat Protoc* 1(2):848–858
20. Fields RD, Stevens-Graham B (2002) New insights into neuron-glia communication. *Science* 298(5593):556–562
21. Hansson E, Ronnback L (2003) Glial neuronal signaling in the central nervous system. *FASEB J* 17(3):341–348
22. Inoue K (2002) Microglial activation by purines and pyrimidines. *Glia* 40(2):156–163
23. Burnstock G (2007) Physiology and pathophysiology of purinergic neurotransmission. *Physiol Rev* 87(2):659–797
24. Burnstock G, Krugel U, Abbracchio MP, Illes P (2011) Purinergic signalling: from normal behaviour to pathological brain function. *Prog Neurobiol* 95(2):229–274
25. Burnstock G (2015) Physiopathological roles of P2X receptors in the central nervous system. *Curr Med Chem* 22(7):819–844
26. Sun L, Gao J, Zhao M, Cui J, Li Y, Yang X et al (2015) A novel cognitive impairment mechanism that astrocytic p-connexin 43 promotes neuronal autophagy via activation of P2X7R and down-regulation of GLT-1 expression in the hippocampus following traumatic brain injury in rats. *Behav Brain Res* 291:315–324
27. Zimmermann H, Braun N (1999) Ecto-nucleotidases—molecular structures, catalytic properties, and functional roles in the nervous system. *Prog Brain Res* 120:371–385
28. Filippini A, Taffs RE, Agui T, Sitkovsky MV (1990) Ecto-ATPase activity in cytolytic T-lymphocytes. Protection from the cytolytic effects of extracellular ATP. *J Biol Chem* 265(1):334–340
29. Sikora A, Liu J, Brosnan C, Buell G, Chessel I, Bloom BR (1999) Cutting edge: purinergic signaling regulates radical-mediated bacterial killing mechanisms in macrophages through a P2X7-independent mechanism. *J Immunol* 163(2):558–561
30. Ferrari D, Chiozzi P, Falzoni S, Dal Susino M, Collo G, Buell G et al (1997) ATP-mediated cytotoxicity in microglial cells. *Neuropharmacology* 36(9):1295–1301
31. Zhang Z, Chen G, Zhou W, Song A, Xu T, Luo Q et al (2007) Regulated ATP release from astrocytes through lysosome exocytosis. *Nat Cell Biol* 9(8):945–953
32. Beigi R, Kobatake E, Aizawa M, Dubyak GR (1999) Detection of local ATP release from activated platelets using cell surface-attached firefly luciferase. *Am J Phys* 276(1 Pt 1):C267–C278
33. Dubyak GR, el-Moatassim C (1993) Signal transduction via P2-purinergic receptors for extracellular ATP and other nucleotides. *Am J Phys* 265(3 Pt 1):C577–C606
34. Ciccarelli R, Ballerini P, Sabatino G, Rathbone MP, D'Onofrio M, Caciagli F et al (2001) Involvement of astrocytes in purine-mediated reparative processes in the brain. *Int J Dev Neurosci* 19(4):395–414
35. Hoegen T, Tremel N, Klein M, Angele B, Wagner H, Kirschning C et al (2011) The NLRP3 inflammasome contributes to brain injury in pneumococcal meningitis and is activated through ATP-dependent lysosomal cathepsin B release. *J Immunol* 187(10):5440–5451
36. Chavez-Valdez R, Martin LJ, Northington FJ (2012) Programmed necrosis: a prominent mechanism of cell death following neonatal brain injury. *Neuro Res Int* 2012:257563
37. Robson SC, Sevigny J, Zimmermann H (2006) The E-NTPDase family of ectonucleotidases: structure function relationships and pathophysiological significance. *Purinergic Signal* 2(2):409–430
38. Abbracchio MP, Burnstock G (1994) Purinoceptors: are there families of P2X and P2Y purinoceptors? *Pharmacol Ther* 64(3):445–475
39. Burnstock G (2008) Purinergic signalling and disorders of the central nervous system. *Nat Rev Drug Discov* 7(7):575–590
40. Collo G, Neidhart S, Kawashima E, Kosco-Vilbois M, North RA, Buell G (1997) Tissue distribution of the P2X7 receptor. *Neuropharmacology* 36(9):1277–1283
41. Jimenez-Pacheco A, Mesuret G, Sanz-Rodriguez A, Tanaka K, Mooney C, Conroy R et al (2013) Increased neocortical expression of the P2X7 receptor after status epilepticus and anticonvulsant effect of P2X7 receptor antagonist A-438079. *Epilepsia* 54(9):1551–1561
42. Ryu JK, McLarnon JG (2011) Block of purinergic P2X(7) receptor is neuroprotective in an animal model of Alzheimer's disease. *Neuroreport* 19(17):1715–1719
43. Kim JE, Ryu HJ, Yeo SI, Kang TC (2010) P2X7 receptor regulates leukocyte infiltrations in rat frontoparietal cortex following status epilepticus. *J Neuroinflammation* 7:65
44. Peng W, Cotrina ML, Han X, Yu H, Bekar L, Blum L et al (2009) Systemic administration of an antagonist of the ATP-sensitive receptor P2X7 improves recovery after spinal cord injury. *Proc Natl Acad Sci U S A* 106(30):12489–12493
45. Sharp AJ, Polak PE, Simonini V, Lin SX, Richardson JC, Bongarzone ER et al (2008) P2X7 deficiency suppresses development of experimental autoimmune encephalomyelitis. *J Neuroinflammation* 5:33
46. Wang YC, Cui Y, Cui JZ, Sun LQ, Cui CM, Zhang HA et al (2015) Neuroprotective effects of brilliant blue G on the brain following traumatic brain injury in rats. *Mol Med Rep* 12(2):2149–2154
47. MacKenzie A, Wilson HL, Kiss-Toth E, Dower SK, North RA, Surprenant A (2001) Rapid secretion of interleukin-1beta by microvesicle shedding. *Immunity* 15(5):825–835
48. Xiang Z, Chen M, Ping J, Dunn P, Lv J, Jiao B et al (2006) Microglial morphology and its transformation after challenge by extracellular ATP in vitro. *J Neurosci Res* 83(1):91–101
49. Li J, Li X, Jiang X, Yang M, Yang R, Burnstock G et al (2017) Microvesicles shed from microglia activated by the P2X7-p38

- pathway are involved in neuropathic pain induced by spinal nerve ligation in rats. *Purinergic Signal* 13(1):13–26
50. Raposo G, Stoorvogel W (2013) Extracellular vesicles: exosomes, microvesicles, and friends. *J Cell Biol* 200(4):373–383
 51. Davalos D, Grutzendler J, Yang G, Kim JV, Zuo Y, Jung S (2005) ATP mediates rapid microglial response to local brain injury in vivo. *Nat Neurosci* 8(6):752–758
 52. Ferrari D, Pizzirani C, Adinolfi E, Lemoli RM, Curti A, Idzko M et al (2006) The P2X7 receptor: a key player in IL-1 processing and release. *J Immunol* 176(7):3877–3883
 53. Bachstetter AD, Rowe RK, Kaneko M, Goulding D, Lifshitz J, Van Eldik LJ (2013) The p38alpha MAPK regulates microglial responsiveness to diffuse traumatic brain injury. *J Neurosci* 33(14):6143–6153
 54. Mullershausen F, Zecri F, Cetin C, Billich A, Guerini D, Seuwen K (2009) Persistent signaling induced by FTY720-phosphate is mediated by internalized SIP1 receptors. *Nat Chem Biol* 5(6):428–434
 55. McGraw J, Hiebert GW, Steeves JD (2001) Modulating astrogliosis after neurotrauma. *J Neurosci Res* 63(2):109–115
 56. Sofroniew MV (2009) Molecular dissection of reactive astrogliosis and glial scar formation. *Trends Neurosci* 32(12):638–647
 57. Giulian D, Woodward J, Young DG, Krebs JF, Lachman LB (1998) Interleukin-1 injected into mammalian brain stimulates astrogliosis and neovascularization. *J Neurosci* 8(7):2485–2490
 58. Woiciechowsky C, Schoning B, Stoltenburg-Didinger G, Stockhammer F, Volk HD (2004) Brain-IL-1 beta triggers astrogliosis through induction of IL-6: inhibition by propranolol and IL-10. *Med Sci Monit* 10(9):BR325–BR330